Strongly Anisotropic Band Dispersion of an Image State Located above Metallic Nanowires

I. G. Hill* and A. B. McLean†

Department of Physics, Queen's University, Kingston, Ontario, Canada, K7L 3N6

(Received 10 September 1998)

Indium can be grown on Si(111) in a 4×1 pattern that contains rows of In atoms spaced 13.3 Å apart that have quasi-one-dimensional electronic structure. This ordered array of metallic wires produces an image-induced surface state series. We have measured the dispersion of the most tightly bound ($n = 1$) image state band and found it to be unconventional because it falls below the free electron parabola perpendicular to the In atom rows. The most straightforward explanation for this is that the electrons feel the surface corrugation potential produced by the rows of In atoms. We were able to infer the form of the potential from our measurements. [S0031-9007(99)08625-1]

PACS numbers: 73.20.At, 73.20.Dx

Indium can be grown on Si(111) in a 4×1 pattern [1], that contains long rows of In atoms [2–6] that are either 2 or 3 atoms wide [3] with a center-to-center separation of 13.3 Å. The surface reconstruction is complex and still under active study. Candidate structures conveniently divide into two categories. There are those that place the In atoms on a largely unreconstructed Si(111) surface [3,7,8] and those that require the uppermost Si layer to reconstruct [6]. The electronic structure of the 4×1 phase has also been the subject of intense study. Recent photoemission [9], inverse photoemission [10–12], and STM [4] studies have provided compelling evidence that the 4×1 phase is both quasi-1D and metallic. It is the latter property that sets the 4×1 system apart from other quasi-1D systems like the insulating Si(111)-$M(3 \times 1)$ (where $M = \{$Li, Na, K, and Ag$\}$) overlayer systems [13]. Both photoemission [9] and inverse photoemission [10–12] have detected flat bands perpendicular to the atom rows and a Fermi level crossing in single domain samples at $\approx 0.6\ \overline{\Gamma X}$ parallel to the atom rows. Consequently, the experimental evidence suggests that the 4×1 system may contain the smallest known metallic wires in existence. The possibility of integrating these naturally occurring wires into practical electronic devices remains a dream. However, recent developments in lithography [14] have demonstrated that it should be possible to continue to reduce the size of electronic devices down to the atomic or molecular limit where the wires could be used as atomic scale interconnects.

In the course of our study of the 4×1 system [10–12], we discovered an image-induced surface state located 0.67 ± 0.15 eV below the vacuum level at the $\bar{\Gamma}$ point. Image-induced surface states are spatially confined by both the surface barrier and the long-range image potential [15–17]. What makes these states particularly interesting is that the image potential is associated with electrons in an array of ordered metallic wires that are only a few atoms wide. In fact, the surface structure resembles an atomic scale diffraction grating with a translational symmetry that is quite unlike that of the low index metal surfaces where image states have been extensively studied [18]. Consequently, the form of the surface potential may also be different, and this may modify the free electronlike image state band dispersion that is universally found on metal surfaces [18]. This universal behavior arises from the fact that the image state wave function lies mainly within the vacuum region, where there is usually no appreciable variation in the potential parallel to the surface [19]. Inverse photoemission provides a convenient means of measuring the dispersion of these states. Furthermore, the binding energy of the image state provides a useful probe of the image potential which is ultimately determined by many-body interactions [20]. Although we will not address the nature of the many-body state within the quasi-1D atom rows, we note that recent high resolution photoemission studies of other quasi-1D systems have provided evidence for non-Fermi-liquid-like behavior [21]. The nature of the many-body state within the In rows of the 4×1 system is still an intriguing open question.

The inverse photoemission studies were performed with a low-energy electron gun [22] and a high sensitivity, Geiger-Müller bandpass photon detector [23] that has a bandwidth of 0.6 eV FWHM centered on 10.6 eV. The single domain 4×1 overlayers were grown on vicinal n-type Si(111) wafers that had a resistivity of $\approx 5\ \Omega$ cm. The wafers were miscut by $3° \pm 0.5°$ towards $[\bar{1}\bar{1}2]$. Further details can be found in previous publications [10–12].

In Fig. 1 we show a series of inverse photoemission spectra that were collected from the 4×1 system in the $[\bar{1}10]$ azimuth (hereafter the directions will be defined with respect to the In atom rows of our single domain 4×1 system; i.e., $[\bar{1}10] \rightarrow \parallel$ and $[\bar{1}\bar{1}2] \rightarrow \perp$). The lower spectrum was collected with the electron gun in normal incidence and all points on the experimental curve probe the $\bar{\Gamma}$ point of the surface Brillouin zone. The state located 0.67 ± 0.15 eV below the vacuum level is the $n = 1$ image state [10,24,25]. As the electron gun is moved off-normal, the state disperses towards the

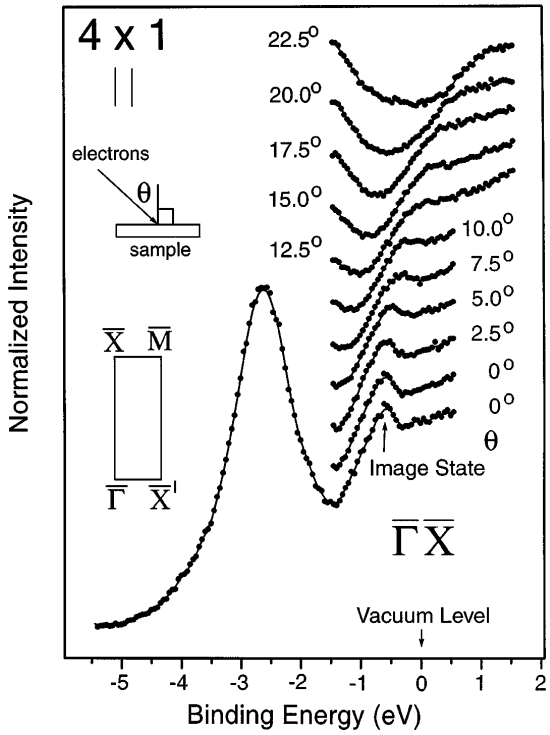

FIG. 1. Si(111)-In(4×1): Inverse photoemission spectra collected in the $\|$ direction ($\bar{\Gamma}\bar{X}$). The angles indicate the position of the electron gun relative to the surface normal in degrees.

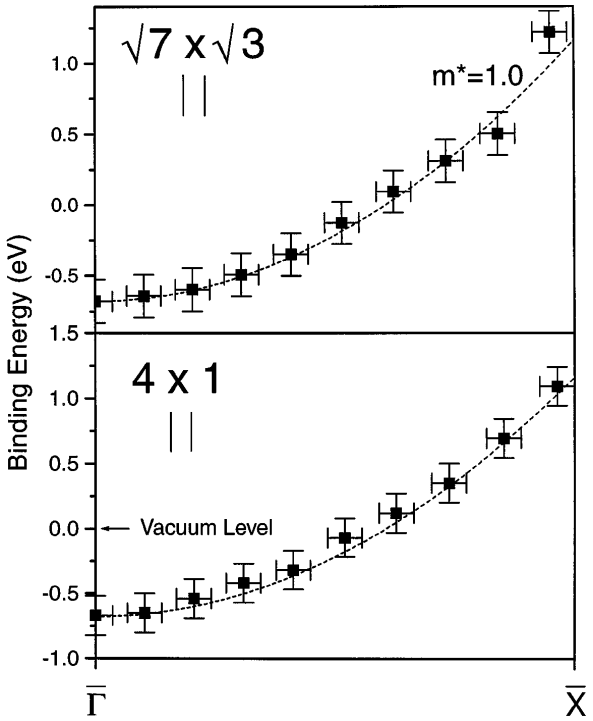

FIG. 2. The dispersion of the $n = 1$ image state in the quasi-2D Si(111)-In($\sqrt{7}$) system (upper panel) is compared with the dispersion of the corresponding state in the quasi-1D Si(111)-In(4×1) system (lower panel) along the $\|$ direction ($\bar{\Gamma}\bar{X}$). The dispersion of both states is described very well by a free electron parabola matched to the experimental curves at $\bar{\Gamma}$.

vacuum level. To obtain good counting statistics, only the energy range around the image state was studied. The features at higher binding energy have been discussed in detail in previous publications [10–12]. To obtain precise estimates of the binding energy, a Gaussian function was superimposed on a quadratic background and fit to the experimental spectra. This simple procedure works well and it can be justified on the grounds that the experimental resolution is large compared with the linewidth of the image state and the transfer function of the detector is fairly symmetric [26]. The contact potential between the electron gun and the sample was also measured during the course of the experiment, and corrections were made for contact potential changes.

We will also present some measured image state dispersions from the higher coverage ($\approx$1 ML) quasi-2D $\sqrt{7} \times \sqrt{3}$ system (hereafter $\sqrt{7}$) to illustrate the striking difference between the two systems. Ignoring the finer details of the $\sqrt{7}$ surface reconstruction, STM studies have revealed [5] that the spaces between the rows of In atoms have now been filled and the surface is reconstructed. Consequently, we would not expect the magnitude of the surface corrugation potential to be substantially different along the $\|$ and $\perp$ directions. In the upper panel of Fig. 2, the dispersion of the image state in the $\sqrt{7}$ system has been plotted in the extended zone representation along the $\|$ direction. The dotted line is a free electron parabola which has been matched to the experimental data at the $\bar{\Gamma}$ point [setting $m_e \rightarrow 1$ and $\hbar \rightarrow 1$; $\varepsilon(k) = \frac{1}{2}k^2 - 0.67$ where k lies in the surface plane]. In the lower panel of Fig. 2, the band dispersion of the corresponding image state in the 4×1 system is presented. Again the measured dispersion is described very well by the free electron parabola, suggesting that the corrugation of the surface potential along the atom rows in the plane of image state is weak. Within our experimental resolution ($\pm$0.15 eV), the binding energy of the $n = 1$ band also lies 0.67 eV below the vacuum level.

In Fig. 3 we present the measured image state dispersions along the $\perp$ direction in the reduced zone representation. In contrast to the data presented in Fig. 2, the dispersion of the image state in the two systems is now quite different. Although the band dispersion in the quasi-2D $\sqrt{7}$ system is again described exceptionally well by $\frac{1}{2}k^2 - 0.67$, the dispersion of the 4×1 image state falls below this curve. Furthermore, although the experimental dispersion is no longer parabolic (in the extended zone representation, there is a clear discontinuity in the slope of the band at $\bar{X}'$), fitting a quadratic to the experimental bands yields an effective mass of $1.4m_e$, which indicates how much the band is contracted by the surface potential.

The most straightforward explanation for this behavior is that the magnitude of the surface corrugation potential in the 4×1 system perpendicular to the rows of atoms is

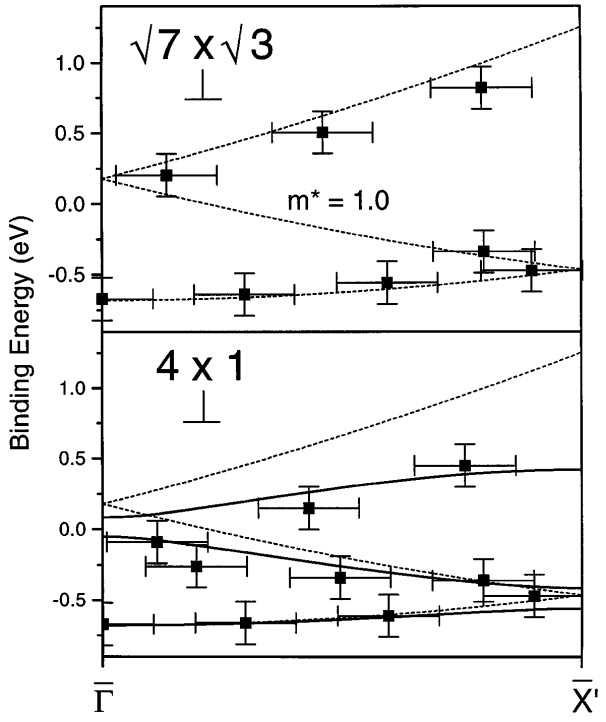

FIG. 3. As for Fig. 2, but in the $\perp$ direction. The dispersion of the image state in the $\sqrt{7}$ system is free electronlike. In contrast, the dispersion of the image state in the 4×1 system falls below the free electron parabola (dotted line) in the upper two bands. The full line was obtained by solving the 1D Schrödinger equation as described in the text.

very large. Although, we would not expect the surface corrugation within the atom chains to be substantially different from the surface corrugation on a metal surface, the surface corrugation potential perpendicular to the wires could, in principle, be much larger. This suggestion is supported by published STM images and line scans [2,3,5,27] which indicate that the local density of states, albeit below the energy of the image state, near the Fermi level is strongly corrugated perpendicular to the In atom chains. A fascinating line scan taken across a $4 \times 1/\sqrt{7}$ phase boundary clearly shows the surface corrugation almost vanishes above the $\sqrt{7}$ phase [5].

The magnitude of the corrugation potential can actually be inferred from the measured energy bands by expressing both the image state wave function and the surface corrugation potential as a Fourier series and converting the 1D Schrödinger equation to a set of simultaneous equations (that are described by the "central" equation [28]). The energy eigenvalues of the resulting set of linear equations were established in analytical form using symbolic computer algebra [29,30]. The potential was altered in *ad hoc* fashion until the calculated bands agreed with the experimental bands. Our main finding is that although the first two minigaps are small (see Fig. 3) the third and fourth (not shown) are large. The surface potential (in eV) used to generate the energy bands that are presented in Fig. 3 is

$$V(x) = 1.07 \sin G_3 x + 0.41 \cos G_4 x , \qquad (1)$$

where $G_n = n2\pi/a$ and $a = 13.3$ Å. This potential has two deep minima separated by $\approx$4.2 Å (see Fig. 4). STM line profiles taken perpendicular to the atom rows in positive bias possess two maxima that are also separated by 4.2 Å [27]. Furthermore, recent surface x-ray diffraction studies have determined that the In atom rows are two atoms wide and the spacing between the In atoms is $\approx$4.5 Å [31]. All three experiments are clearly probing the internal structure of the In atom rows.

Because the energy eigenvalues were determined exactly (not using nearly free-electron theory), the first two minigaps are finite even though the coefficients of terms containing G_1 and $G_2 = 0$. Although it was relatively easy to determine the magnitude of the third and fourth Fourier components, it was not possible for us to determine the first two components of the Fourier series because we were unable to resolve symmetry split states at the high symmetry points of the lower two bands. However, the good agreement between the calculated and measured bands suggests that the surface potential does influence the image state dispersion. This behavior has been observed before, but only at a zone boundary. Spin-polarized inverse photoemission measurements of Co(10$\bar{1}$0) have recently found evidence for a large (0.6 eV) symmetry splitting of the $n = 1$ image state at the $\bar{Y}$ zone boundary [32]. In our experiments, we have not been able to resolve symmetry split image states at the superlattice zone boundary. However, our calculations indicate that the size of the first two minigaps should be much smaller than 0.6 eV (Fig. 3). Consequently, we are unable to resolve the two components, and it is more likely that we have measured a weighted average of the two symmetry split states at the zone boundary. This may explain why the binding energy of the lowest lying band is so close to the free electron parabola near $\bar{X}'$.

We have measured the dispersion of the $n = 1$ image state band above an ordered array of metallic atom rows and found it to be strongly anisotropic. Along the atom rows (and also in the 2D $\sqrt{7}$ system) m^* is close to unity, demonstrating that we have excellent

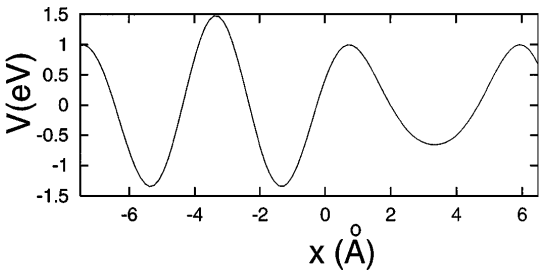

FIG. 4. The function $V(x)$ has two minima separated by $\approx$4.2 Å.

momentum resolution [33]. Perpendicular to the rows, the dispersion of the state is unconventional, falling below the "universal" free electron parabola [18]. In the extended zone representation, there is a clear change in slope at the $\times 4$ superlattice wave vector ($\bar{X}'$). This unambiguously implicates the surface potential as the source of the band perturbation. The potential extracted from a 1D band calculation has two pronounced minima spaced 4.2 Å apart in excellent agreement with STM line profiles measured at lower energy and also with recent surface x-ray diffraction studies. The 4×1 image state is particularly interesting because it is partially delocalized, lying intermediate between the fully localized image state recently discovered at step edges on Cu(100) [34] and the ubiquitous free electronlike image states found on metal surfaces.

The Natural Sciences and Engineering Research Council of Canada is thanked for financial support. Malcolm Stott is also thanked for his critical reading of this manuscript.

*Present address: Department of Electrical Engineering, Princeton University, Princeton, NJ 08544

†Author to whom correspondence should be addressed.

[1] M. Kawaji, S. Baba, and A. Kinbara, Appl. Phys. Lett. **34**, 748 (1979).
[2] S. Park, J. Nogami, and C. F. Quate, J. Microsc. **152**, 727 (1988).
[3] J. L. Stevens, M. S. Worthington, and I. S. T. Tsong, Phys. Rev. B **47**, 1453 (1993).
[4] J. Kraft, M. G. Ramsey, and F. P. Netzer, Phys. Rev. B **55**, 5384 (1997).
[5] J. Kraft, S. L. Survnev, and F. P. Netzer, Surf. Sci. **340**, 36 (1995).
[6] A. A. Saranin *et al.*, Phys. Rev. B **56**, 1017 (1997).
[7] N. Nakamura, K. Anno, and S. Kono, Surf. Sci. **256**, 129 (1991).
[8] D. M. Cornelison, M. S. Worthington, and I. S. T. Tsong, Phys. Rev. B **43**, 4051 (1991).
[9] T. Abukawa *et al.*, Surf. Sci. **325**, 33 (1995).
[10] I. G. Hill and A. B. McLean, Phys. Rev. B **56**, 15 725 (1997).
[11] I. G. Hill and A. B. McLean, Appl. Surf. Sci. **123/124**, 371 (1998).
[12] I. G. Hill, Ph.D. thesis, Queen's University, 1997.
[13] D. Jeon, T. Hashizume, T. Sakurai, and R. F. Willis, Phys. Rev. Lett. **69**, 1419 (1992).
[14] M. F. Crommie, C. P. Lutz, and D. M. Eigler, Science **262**, 218 (1993).
[15] V. Dose *et al.*, Phys. Rev. Lett. **52**, 1919 (1984).
[16] P. M. Echenique and J. B. Pendry, J. Phys. C **11**, 2065 (1978).
[17] N. V. Smith, Phys. Rev. B **32**, 3549 (1985).
[18] D. Straub and F. J. Himpsel, Phys. Rev. B **33**, 2256 (1986).
[19] P. M. Echenique and M. E. Uranga, Surf. Sci. **247**, 125 (1991).
[20] M. Nekovee and J. E. Inglesfield, Prog. Surf. Sci. **50**, 149 (1995).
[21] B. Dardel *et al.*, Phys. Rev. Lett. **67**, 3144 (1991).
[22] P. W. Erdman and E. C. Zipf, Rev. Sci. Instrum. **53**, 225 (1982).
[23] I. G. Hill and A. B. McLean, Rev. Sci. Instrum. **69**, 261 (1998).
[24] H. Öfner, S. L. Surnev, Y. Shapira, and F. P. Netzer, Phys. Rev. B **48**, 10 940 (1993).
[25] H. Öfner, S. L. Surnev, Y. Shapira, and F. P. Netzer, Surf. Sci. **307–309**, 315 (1994).
[26] K. Prince, Rev. Sci. Instrum. **59**, 741 (1988).
[27] J. Nogami, S. Park, and C. F. Quate, Phys. Rev. B **36**, 6221 (1987).
[28] C. Kittel, *Introduction to Solid State Physics* (John Wiley and Sons, New York, 1976).
[29] MAPLE, Waterloo Maple Inc., Waterloo, Ontario, Canada.
[30] I. G. Hill and A. B. McLean, Comput. Phys. (to be published).
[31] O. Bunk *et al.*, Phys. Rev. B (to be published).
[32] S. Bode, K. Starke, P. Rech, and G. Kaindl, Phys. Rev. Lett. **72**, 1072 (1994).
[33] S. Yang, K. Garrison, and R. A. Bartynski, Phys. Rev. B **43**, 2025 (1991).
[34] J. E. Ortega, F. J. Himpsel, R. Haight, and D. R. Peale, Phys. Rev. B **49**, 13 859 (1994).